X-RAY IMAGING TECHNIQUE SIMPLIFIES AND IMPROVES RESERVOIR-CONDITION UNSTEADY-STATE RELATIVE PERMEABILITY MEASUREMENTS

D. R. Maloney, Phillips Petroleum Company

ABSTRACT

This paper describes an x-ray imaging technique that has been successfully employed to simplify and improve one of the most basic (and potentially most error-prone) laboratory measurements required for calculating relative permeability functions from unsteady-state core flood data - namely the measurement of fluid production and saturation history.

Typically, during conventional unsteady-state core tests, fluids that are produced from a core travel through some distance of tubing downstream from the core before reaching the device that measures or infers produced fluid volumes. Because production is normally measured downstream from the outlet face of the core, a number of corrections are necessary to compensate for upstream and downstream tubing volume, time lag between when fluids exit the core and when they are measured or observed, and any volume changes that occur because of differences in pressure and temperature at the point of measurement compared to core conditions. Measurement complexity and potential for errors increase when produced fluids do not separate quickly. Thus, potential sources of error include how data is corrected as well as how production is measured. Obviously, data errors yield imprecision in relative permeability results.

By acquiring x-ray images of the entire core at various times during a coreflood using an x-ray image intensifier or similar type of device, one gains real time data describing bulk saturation changes within a core. This data is processed to yield volumetric data for input in conventional unsteady-state relative permeability calculations. Production data does not need to be time corrected as it directly reflects fluid saturation changes within the core plug during times that directly match those of pressure measurements. The technique greatly simplifies reservoir condition tests even when produced fluids separate slowly or are in the form of emulsions. Examples from reservoir condition tests are provided to demonstrate the technique.

INTRODUCTION

Unsteady-state relative permeability tests are performed by measuring fluid production and pressure gradient with time as a displacing fluid is injected into a core plug under conditions of constant pressure or constant flow rate. Data results are processed to determine relative permeability versus saturation functions. One of the most error-prone aspects of the unsteady-state test is measurement of fluid production and saturation history. The next 2 sections describe production monitoring and in situ saturation techniques as background for comparison with the imaging technique described in this paper.

Production Monitoring
When volumetric or mass balance techniques are used to determine saturation changes in cores, corrections to the test data are necessary to account for non-core fluid volumes displaced from upstream and downstream tubing and for differences between times when fluids are produced from a core and when production is observed in a measuring system downstream from the core.

Figure 1 is provided for illustrative purposes. Assume that one uses this simple configuration for a brine-displacing-oil unsteady-state relative permeability test. Figure 1a represents oil injection immediately prior to starting brine injection. Upstream and downstream tubing are filled with oil. In Figure 1b, the upstream valve is rapidly switched to begin brine flow. However, brine doesn't reach the upstream core face until Figure 1c.

Between Figures 1c and 1d, brine invades the core plug, saturation and pressure gradients change, but the first drop of oil replaced by brine within the core plug (black dot) has yet to be produced from the downstream tubing. For test results to accurately reflect saturation changes in the core, production data has to be corrected to account for oil that was produced from upstream and downstream tubing.

Between Figures 1d and 1e, the brine flood progresses. In Figure 1e, brine has reached the downstream core face and will begin to be produced into the downstream tubing. Subsequent data will be critical for traditional unsteady-state relative permeability calculations, yet brine production is still not observed until after 1f, when the first drop of brine finally reaches the end of the downstream tubing and enters the production-measurement system. Note that to correlate core production time with pressure gradient time, production of Figure 1f is matched to pressure gradient of Figure 1e. Production history has to be time-corrected so that it tracks on the same time-scale as pressure history. Obviously, data errors yield imprecision in relative permeability results.

Classic techniques for ambient temperature tests with fluid production at atmospheric temperature include the use of calibrated glass capture vessels in which an operator notes produced fluid volumes at various times throughout a test. For simple tests with fluids that separate immediately, volumetric measures are relatively straightforward, albeit tedious, but loose effectiveness as test conditions become more challenging or as fluids don't separate quickly. During the past decade, investigators have described semi-automated data collection schemes such as capturing liquids in containers on digital balances [1, 2, 3]. Mass-balance techniques are inaccurate when densities of produced fluids are similar. Such techniques also have shortcomings when measurements recorded at one set of conditions (temperature and pressure) are used to infer production at another set of conditions. Acoustically monitored separators [4] and x-ray monitored separators [5] offer advantages for tests with elevated pore pressure. However, methods that infer production from changes in produced fluid interface levels within a downstream separator loose accuracy when fluids do not separate immediately when produced.

In Situ Saturation Monitoring

Measuring in situ saturation changes during core floods by an energy absorption technique such as x-ray CT scans, linear x-ray scans, or gamma ray scans is becoming common [6]. Saturation changes within the rock are measured directly. Limitations depend upon the measurement method employed and the rate at which saturation changes within the core plug. Several gamma ray and x-ray scan methods employ a stop-measure-move approach to obtain data at a number of discrete positions along the core to describe a saturation profile. During unsteady-state tests with rapidly changing saturation, such techniques may be too slow to adequately capture core saturation throughout the core at an instant of time. Another consideration is the complexity of the data processing technique. Ideally one would like to use a technique whereby saturations can be calculated from in situ measurement techniques with a minimum amount of data processing complexity.

SIMPLE IN SITU SATURATION IMAGING TECHNIQUE

The x-ray imaging techniques of the rest of this paper were devised to measure bulk saturation within a core plug at an instant of time. By comparing changes in core images with time, one can infer production from the core plug.

Scanner

The scanner (Figure 2) consists of x-ray tube and detector platforms that move on opposite sides of a center sample rack. Experiments are mounted on the center rack. The portion of the rack that can be x-ray scanned is 1.3 m high by 3.1 m long. The tube and detector platforms move parallel (horizontal and vertical) and perpendicular (in and out) to the sample rack. The tube and detector platforms are coupled so that they always move together horizontally. Each platform is moved in the vertical direction by its own stepper motor. During normal vertical axis movements, travel for both platforms is synchronized such that the x-ray beam and image intensifier remain aligned. Each platform has its own stepper motor for movement inward or outward from the sample rack - from about 4 cm from the sample rack for both platforms to 85 cm for the tube and 76 cm for the detector (161 cm maximum distance between the tube and detector). For all axes, position resolution is 0.1 mm. Moving the image intensifier outward from a sample enlarges the x-ray image of the sample. When cores are 14 cm long or less, as is typical when performing unsteady-state relative permeability tests on single core plugs, the entire core can be imaged in one “shot”. Longer cores require combining multiple images to build a composite image.

The scanner uses a 165 kVp dual-focus metal ceramic x-ray tube. A 0.4 mm focus is used for imaging. The tube potential can be varied from 7.5 kVp to 160 kVp. Tube current can be varied from 0.5 to 5 mA with the 0.4 mm focus. The tube-head shield includes a lead shutter that opens when an exposure is in progress and closes afterwards. The x-ray detector used for these measurements is an Applied Optics Model PS92 image intensifier with CCD video camera output. The video camera has an automatic gain correction feature that adjusts image brightness when illumination of an object becomes too dim or too bright. This feature had to be turned off to prevent the camera from automatically adjusting image brightness. Horizontal and vertical shutters immediately in front of the image intensifier are adjusted to mask the image intensifier. For example, Figure 2 includes an x-ray image of a core within a coreholder. Considering the core image of Figure 2, typically the shutters would be adjusted to mask the bright regions on either side of the core for subsequent scans. Masking also protects the image intensifier from high x-ray exposure that would decrease the useful life of the imaging device. Image acquisition and scanner operations are controlled from a laboratory PC that is located outside of the lead-lined x-ray room. Further details are described elsewhere [5].

X-Ray Images

When x-rays pass through a sample, such as a core within a coreholder, and onto the image intensifier, video output from the image intensifier provides a real-time x-ray image of the sample. When the core is saturated with fluids of different x-ray absorption characteristics, a change in saturation within the core causes a change in grey-scale intensity of the x-ray image in portions of the rock affected by the saturation change. For gas-liquid systems, it is possible to resolve gas and liquid saturations without adding an x-ray absorber to the liquid phase, although contrast significantly improves when an absorber or x-ray dope is added to the liquid. For oil-brine systems, either the oil or brine is doped to improve contrast. Typically, the brine is doped such that an image of a core brightens as the brine content in the core decreases, as shown in the x-ray image of Figure 3. The x-ray image of Figure 3 was acquired as a brine-saturated core was flooded from below with oil. Output from the image intensifier is displayed on a monitor and is also available to a video capture board within the lab PC. The PC board acquires digital images of 8-bit precision (256 shades of grey). An image consists of 480 rows and 640 columns of pixels. Experience with this system has shown that saturation varies linearly with the natural log of the grey scale intensity. At periodic times during an experiment, image frames are captured to the PC either through a programmed sequence or by manual control (clicking a button on the LabVIEW™ program used to control the x-ray scanner). Although a single image frame can be acquired in about a second, to improve image quality, 20 to100 image frames are typically captured in rapid succession during each imaging event. These frames are averaged to yield a single improved image. This image is saved for subsequent analysis. The time to acquire and average 100 image frames is about 12 seconds.

Image Processing

Typically an image is processed in a LabVIEW™ IMAQ™ application that was written for grey scale pixel value determination. A region of interest is selected that is as long as the core image but 50- 60% of the width of the core image. This is illustrated by the rectangle superimposed on the image of Figure 3. The region of interest is purposefully selected to exclude edge effects where grey scale intensities increase because of sample shape. Within the region of interest, a grey scale intensity profile is constructed along the centerline by averaging pixel values on either side and including the center pixel for a traverse along the long-axis of the core image. The graph on Figure 3 shows a profile for the x-ray image of Figure 3. Subsequently, if grey scale results are to be used to determine saturation profiles, natural log of average grey scale versus position is calculated. Figure 3 also shows an average grey scale value and natural long of average grey scale value for the region of interest. Natural log of average grey scale value, or $Ln(Grey_{avg})$, is used for simple calculation of bulk core saturation.

Experiment Set Up

The following describes experimental practices using restored state oil-brine techniques on samples of known pore volume, focusing on the use of natural log of average grey scale values from a region of interest (described in preceding paragraph) to determine bulk core saturation changes. Although cores can also be tested in native state or with gas-liquid systems, descriptions of such procedures are beyond the scope of this paper.

When starting a series of tests using similar fluids and core plugs, after installing a dry core plug in the coreholder, preliminary x-ray images are acquired to determine physically where to position the x-ray tube and image intensifier to gain adequate x-ray images. Next, either through experience or by comparing x-ray images of a typical core plug when saturated with each test fluid, x-ray tube voltage and current settings are determined to optimize the ability to differentiate between the two fluid phases. Ideally, one would like core images to be dark (grey scale intensities less than 70 but greater than about 25) when the core is saturated with doped fluid and bright (grey scale intensities greater than 200 but less than 255) when the core is completely saturated with the non-doped fluid. The tube voltage is set greater than the excitation potential or *K* absorption edge of the doped fluid. Generally, even though carbon fiber composite coreholders are used to minimize x-ray attenuation caused by the coreholder, the tube is operated with voltage set between 50 kVp and 90 kVp. Tube current is adjusted between 1 and 5 mA to achieve proper image brightness. After reasonable values for tube potential and current have been found, these settings are kept constant throughout an experiment.

Experimental Sequence and Measurements

This section describes using x-ray images of the entire core to determine core saturations during unsteady-state oil-brine tests. Primary test measurements include $Ln(Grey_{avg})$ from x-ray image analysis, pressure gradient, and injected fluid volume versus time.

After determining the brine permeability of the brine-saturated core at test conditions, the core is x-ray imaged. The value of $Ln(Grey_{avg})$ for the brine-saturated core image is determined. X-ray images are periodically recorded after injection is switched from live brine to live oil. For some time after switching from brine to constant-rate oil injection, oil displaces brine from tubing upstream from the core. Brine displaced from the upstream tubing flows through the core. If the volume of brine displaced from the upstream tubing is sufficiently large, because the core is still completely saturated with brine, the pressure gradient across the core plug will stabilize in response to the rate at which oil pushes brine from the upstream tubing. From x-ray images, $Ln(Grey_{avg})$ does not change until oil reaches the inlet core face and begins to penetrate the core.

Typically, when oil begins to penetrate the core, both pressure gradient and $Ln(Grey_{avg})$ begin to change noticeably. A correction for upstream tubing volume, or compensation for the volume of oil injected that simply flushed brine from upstream tubing rather than from the core, consists of "zeroing" time and volume of oil injected at the time when $Ln(Grey_{avg})$ begins to change as a result of the onset of oil penetration into the core.

As oil displaces brine from the core, but before oil breaks through the downstream core face into the downstream tubing, oil that is injected into the core replaces an equivalent volume of brine within the core. Because the x-ray absorption properties of the brine and oil are different, $Ln(Grey_{avg})$ changes linearly with respect to the volume of oil injected into the core. Data from this portion of the oil flood is used to correlate $Ln(Grey_{avg})$ to core saturation. $Ln(Grey_{avg})$ versus injected oil volume data is fit with a linear equation. Next, the linear equation is solved using the pore volume of the core as input. This step determines the value of $Ln(Grey_{avg})$ that would occur if the core were completely saturated with oil. Using $Ln(Grey_{avg})$ values for conditions of 100% brine saturation and 100% oil saturation, a linear equation describing brine saturation as a function of $Ln(Grey_{avg})$ is easily determined. This equation is subsequently used to determine brine saturation from x-ray images acquired at any time during the oil flood or subsequent waterflood. Note that because this x-ray imaging technique does not rely on fluid production measurements, downstream tubing corrections are not necessary. Another advantage is that x-ray images are recorded at the same time as pressure gradient measurements, alleviating the need to compensate for time lags between when fluids are produced from the core and when they can be observed downstream from the core.

Following the oil flood, after the oil permeability for the residual brine saturation condition has been determined and the core has been "aged", the core is ready for the unsteady-state brine-displacing-oil test. Immediately before the brine flood to residual oil saturation and throughout the brine flood, pressure gradient history, injected brine volume versus time, and $Ln(Grey_{avg})$ versus time are recorded. As with the oil flood, until brine displaces oil from the upstream tubing and begins to enter the core, $Ln(Grey_{avg})$ remains constant. Thereafter, until brine breaks through the outlet end of the core, $Ln(Grey_{avg})$ varies linearly with volume of brine injected. After breakthrough, the change in $Ln(Grey_{avg})$ with change in volume of brine injected diminishes as the core approaches a residual oil saturation condition. Because unsteady-state relative permeability calculation methods typically use post-breakthrough data to determine relative permeabilities, the rate at which images are acquired can be increased immediately after breakthrough and decreased later as the saturation state of the core approaches residual oil condition. Late in the test, the flow rate can be increased to "bump" the saturation. Brine saturations are calculated directly from $Ln(Grey_{avg})$. Knowing the difference in saturation between two measurement times, one can calculate the volume of oil that has been "drained" or displaced from the core between the two measurement times. The volume of injected fluid that has also been produced can be calculated by subtracting the volume of "drained" fluid from the volume of fluid injected (flow rate * Δtime – Δdrained-fluid saturation * pore volume). The resulting data is ready for unsteady-state relative permeability calculations.

APPLICATION EXAMPLE

The following example is from a series of unsteady state relative permeability tests performed on 4 Berea sandstone cores of 3.81 cm diameter by 12.7 cm length. Live brine containing 2-weight percent potassium chloride and 6-weight percent cesium chloride (x-ray dope) was used for all tests. Two cores were tested with live oil of 18 cP viscosity, while the other two cores were tested with a live oil of 54 cP viscosity. Both oils were from the same offshore reservoir. Test conditions included 140 atm. pore pressure and 54 $^{\circ}$C temperature. Each core plug was jacketed with Teflon heat-shrink tubing, a wrap of 0.07 mm thick Nickel foil, and a rubber sleeve to isolate the core from confining fluid and to prevent gas from diffusing through the core sleeve into the confining fluid. Figure 4 is a simplified schematic of the closed-loop test system. Major components included Quizix™ pumps (brine injection, oil injection, and downstream pressure maintenance), fluid separator, coreholder, in-line viscometer, and pressure transducers. The original intent was to use a volumetric balance method to determine saturation changes within the rock. Ordinarily, this can be done by observing changes in oil-brine interface level within the separator using x-ray images and accounting for fluid volumes elsewhere in the flow system. Such an approach was soon found to be impractical. As shown by the x-ray image of separator fluids in Figure 5, droplets of brine, after falling through the column of live oil within the separator, would rest on the oil-brine interface for several minutes before breaking. The height of the “stack” of brine droplets varied as a function of brine production rate. This phenomenon negated the potential for accurately using oil-brine interface levels to infer produced fluid volumes. As an alternative, to accomplish project goals, the core plug imaging technique was developed.

Figure 6 shows x-ray images of a core plug as it was flooded with oil to residual brine saturation. As oil (lower x-ray absorption) replaces brine (higher x-ray absorption) within the core, affected portions of the core images change from darker to lighter shades of grey. Figure 7a provides early-time data from the oil flood. Note that $Ln(Grey_{avg})$ varies linearly with volume of oil injected until oil breaks through, or begins to be produced from the core plug. After break-through, the trend “bends over” and begins to flatten. The linear fit to the early-time data is shown on the figure. This equation was used to calculate $Ln(Grey_{avg})$ corresponding to 100% oil saturation by using the pore volume of the core as input. Using this result and that for conditions of 100% brine saturation, a linear correlation between $Ln(Grey_{avg})$ and average core saturation was developed. This correlation was used to easily calculate average core saturation from images acquired during the oil flood and subsequent waterflood.

Figure 7b shows saturation versus time as the core was flooded with oil to S_{wr} at a rate of 0.2 cm^3/minute and later after the oil injection rate was increased several times. With the 0.2 cm^3/minute rate, the brine droplet “stacking” effect of Figure 5 was not too severe, so produced brine volume versus time could be determined with reasonable accuracy by measuring changes in oil-brine interface level within the separator. Accuracy of separator measurements decreased after increasing the oil injection rate. Results from separator (Sepr) measurements are compared with those from the core imaging technique (Core) in Figure 7b. The core image analysis technique provided better accuracy and less scatter compared to the volumetric measurements. It is noteworthy to mention that correcting the volumetric production data (from interface level changes in the separator) for fluid volume changes in upstream and downstream tubing and elsewhere in the flow system and correcting production history to follow the same time scale as pressure history was non-trivial. Because the volume of the tubing between the separator and downstream face of the core was 9 cm^3, it wasn't until 45 minutes after oil broke through the downstream face of the core that oil production was observed in the separator! As a result, pressure gradient history preceded volumetric observations of production by 45 minutes. In contrast, using the core imaging technique, pressure gradient history and saturation history followed the same time scale without need for timing corrections.

Figure 8a shows oil production and pressure response from one of the brine-displacing-oil unsteady state tests. Initial brine injection rate was 1.0 cm^3/minute. Relative permeability versus saturation results were calculated using the Jones-Roszelle [7] method as implemented in a commercially available software product [8]. Unsteady-state results for the 4 core tests are shown on Figure 8b. The results show good consistency.

CONCLUSIONS

The x-ray imaging technique described in this paper simplifies and improves unsteady-state relative permeability measurements, especially when tests are conducted at reservoir conditions with live fluids. Advantages gained from the core plug image analysis technique include the following:

a) Correction for upstream tubing volume is trivial. Downstream tubing volume corrections are not necessary.
b) Saturation measurements from core images are obtained at same times as pressure gradient measurements, requiring no time corrections.
c) Saturation measurements track along the same time-scale as volumes of fluids injected after a simple correction for upstream tubing volume.
d) In situ core saturation measurements are not affected by whether or not fluids form emulsions or separate quickly.

Other types of imaging devices, such as flat panel detectors and array detectors may work as well or better than the image intensifier employed in this investigation. A limitation of the method is that the imaging technique calculates saturation changes within a "region of interest," assuming that the region of interest is completely representative of saturation changes throughout the core plug. The degree to which a region of interest is representative of the entire core plug depends upon the homogeneity of the plug. For a highly heterogeneous core plug, the "appropriateness" of measuring saturation changes only in a region of interest needs to be verified. Typically, however, such core plugs are not suitable for standard unsteady-state relative permeability tests anyway.

AKNOWLEDGMENTS
Appreciation is expressed to Phillips Petroleum Company for supporting this work and allowing this paper to be presented. Thanks are extended to George Dixon, Jeff Johnson, and Dwayne Snyder of Phillips for assembling the flow system and assisting in performing the tests described in this paper.

REFERENCES

1. Gash, B., R. Volz, G. Potter, and J. Corgan, "The Effects of Cleat Orientation and Confining Pressure on Cleat Porosity, Permeability and Relative Permeability in Coal." Paper SCA 9224 presented at the Society of Well Log Analysts and the Society of Core Analysts Symposium, Oklahoma City, OK (June 15-17, 1992).

2. Potter, G. and G. Lyle, "Measuring Unsteady-State Gas Displacing Liquid Relative Permeability of High Permeability Samples." Paper SCA 9419 presented at the 1994 International Symposium of the Society of Core Analysts, Stavanger, Norway (Sept. 12-14, 1994).

3. Maloney, D. and A. Brinkmeyer, "Using A Weight Method for Laboratory Fluid Production Methods." Paper SCA 9306 presented at the 1993 SCA Annual Technical Conference, Houston, TX (Aug. 9-11, 1993).

4. Ebeltoft, E., J. Iversen, K. Vatne, M. Andersen, and J. Nordtvedt, "A Novel Experimental Apparatus for Determination of Three-Phase Relative Permeabilities at Reservoir Conditions." Paper SCA 9636 presented at the 1996 International Symposium of the Society of Core Analysts, Montpellier, France (Sept. 8-10, 1996).

5. Maloney, D., D. Wegener, and D. Zornes, "New X-ray Scanning System for Special Core Analyses in Support of Reservoir Characterization." Paper SCA 9940 presented at the 1999 International Symposium of the Society of Core Analysts, Golden, CO (Aug. 1-4, 1999).

6. Naylor, P. and D. Puckett, "In-Situ Saturation Distributions, The Key to Understanding Core Analysis." Paper SCA 9405 presented at the 1994 International Symposium of the Society of Core Analysts, Stavanger, Norway (Sept. 12-14, 1994).

7. Jones, S. and W. Roszelle, "Graphical Techniques for Determining Relative Permeability from Displacement Experiments." *JPT*, (May, 1978), pp. 807-817.

8. Ruth, D., Portwo, Software Version 10. D&B Ruth Enterprises, Winnipeg, Manitoba.

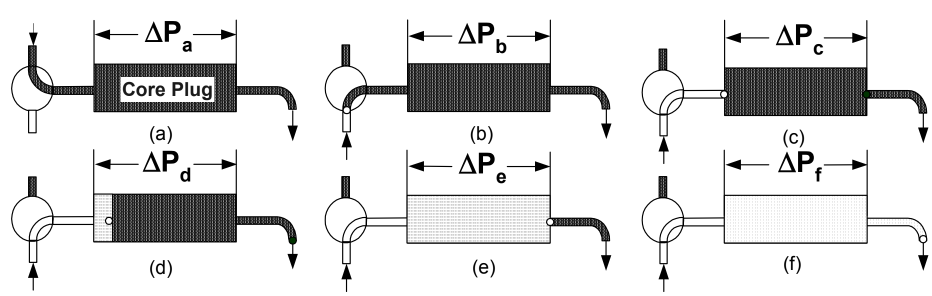

Figure 1. Various stages during a simple brine-displacing-oil unsteady-state test.

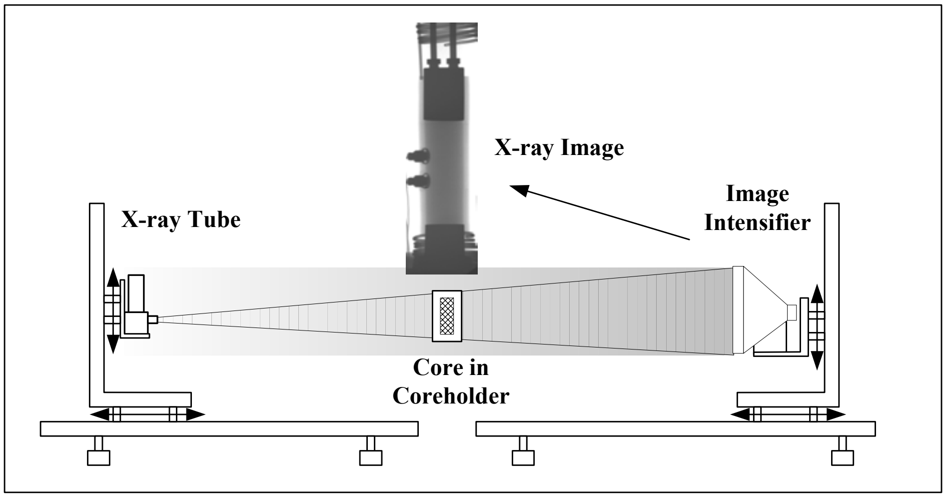

Figure 2. Schematic of x-ray scan arrangement.

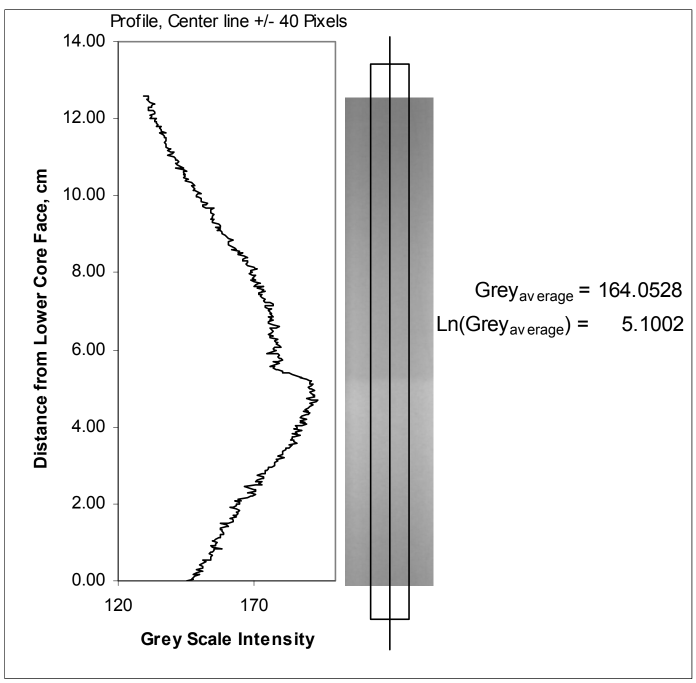

Figure 3. Image analysis.

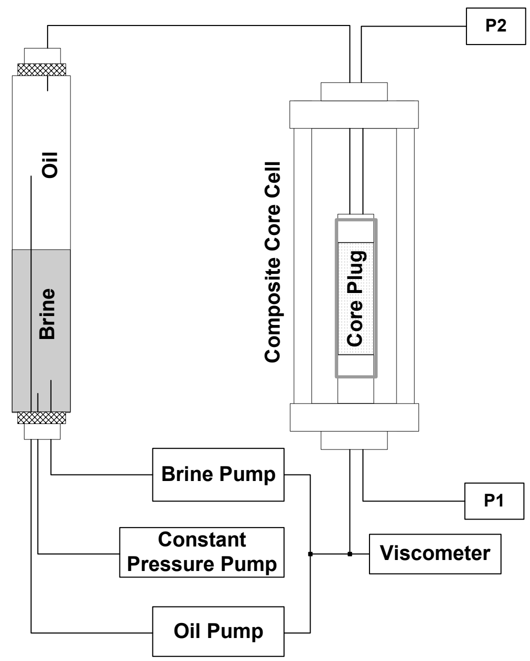

Figure 4. Simplified flow system schematic.

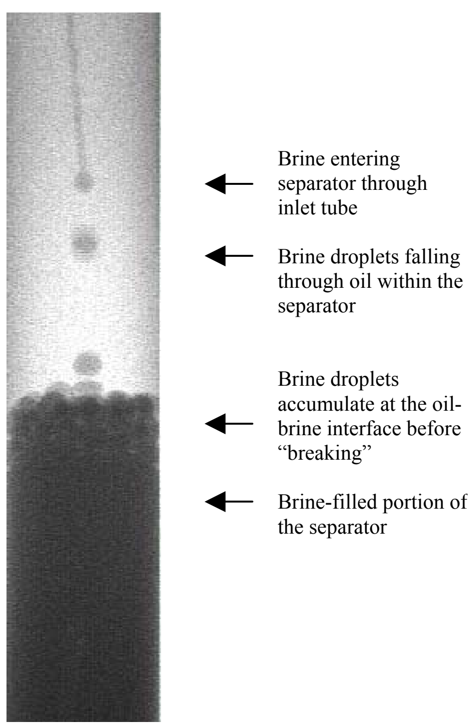

Figure 5. X-ray image of brine droplets accumulating at the oil-brine interface within the fluid separator. Pressure and temperature are 140 atm. and 54 deg. C.

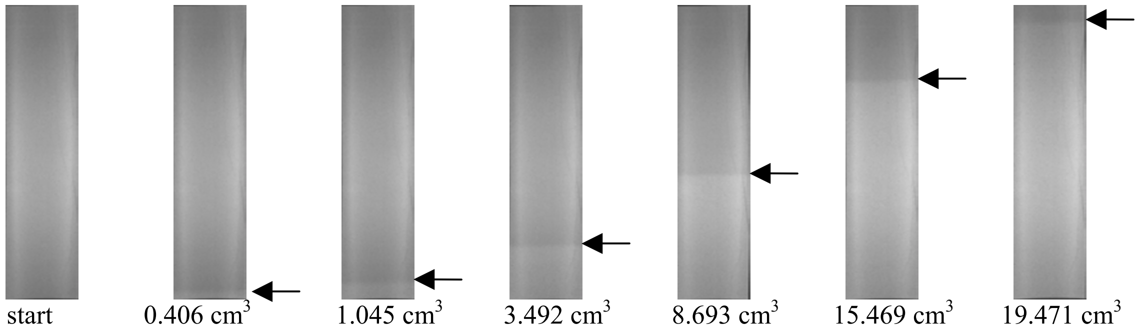

Figure 6. Sequence of x-ray core images. Oil flood with 0.2 cm^3/minute rate.

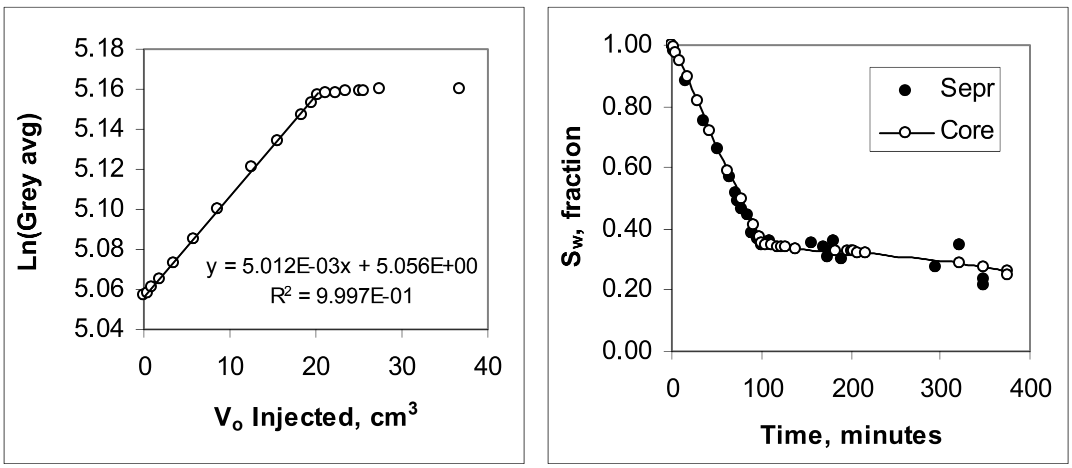

(a) (b)

Figure 7. Oil flood image results. a) Natural log of average grey scale intensity versus oil volume injected. b) Comparison of saturation results from fluid volume changes within the separator (Sepr) and from core image analysis (Core).

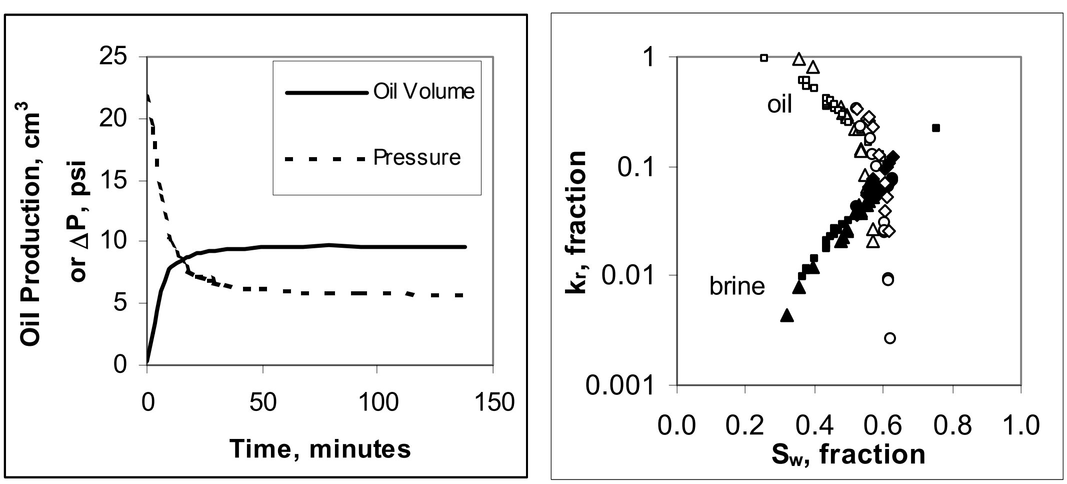

(a) (b)

Figure 8. Unsteady-state brine-displacing oil results. a) Typical oil production and pressure response versus time. b) Relative permeability results from 4 coreflood tests.